ACUSTICA
Vol. 68 (1989)

Oscillations of Bubbles Generated by Imploding and Exploding Hollow Glass Spheres in Liquids

K. Vokurka
Department of Physics, Czech Technical University, Prague, Czechoslovakia

Oscillations of Bubbles Generated by Imploding and Exploding Hollow Glass Spheres in Liquids

Summary

Experimental data found in the literature on oscillations of bubbles generated by imploding and exploding hollow glass spheres in liquids are used to estimate oscillation intensities and the partition of energies in these bubbles. It is found that in the experimental bubbles, in contrast to a theoretical model, excessive dissipation of energy occurs which greatly reduces the intensity of oscillations. The cause of increased energy dissipation and decreased intensity of oscillations is seen in the wall distortion due to glass fragments surrounding the bubble. A distortion factor is introduced to describe the degree of the bubble wall deformation.

Schwingungen von Blasen, die durch implodierende und explodierende hohle Glaskugeln in Flüssigkeiten erzeugt werden

Zusammenfassung

Unter Benutzung experimenteller Literaturdaten über die Schwingungen von Blasen, die durch implodierende und explodierende Glashohlkugeln in Flüssigkeiten entstehen, werden die Schwingungsintensitäten und die Energieaufteilung in den Blasen abgeschätzt. Es zeigt sich, daß in den experimentellen Blasen eine im Vergleich zu theoretischen Vorhersagen außergewöhnlich hohe Energiedissipation auftritt, welche die Intensität der Schwingungen stark vermindern. Der Grund für die erhöhte Energiedissipation und die verminderte Intensität der Schwingungen wird in der Verzerrung der Blasenwand durch Glasfragmente gesehen, welche die Blasen umgeben. Zur Kennzeichnung der Blasendeformation wird ein Verzerrungsfaktor eingeführt.

Les oscillations de bulles engendrées en milieu liquide par l'implosion ou l'explosion de sphères creuses en verre

Sommaire

A partir de données expérimentales déjà publiées concernant les oscillations de bulles engendrées par implosion ou explosion de sphères de verre creuses dans divers liquides, on a effectué des estimations des intensités d'oscillation et de la répartition de l'énergie dans les bulles. Contrairement à un certain modèle théorique, l'analyse des expériences met en évidence un excès de dissipation d'énergie qui se traduit par une réduction rapide de l'amplitude d'oscillation. La cause commune de cette dissipation énergétique accrue et de la décroissance rapide des oscillations est attribuée à la présence de débris de verre sur la paroi de la bulle. On a donc introduit un facteur de distorsion de paroi pour décrire le degré de déformation de la paroi de la bulle.

1. Introduction

Imploding and exploding hollow glass spheres have been used in model experiments on sonoluminescence [1, 2], as a source of impulsive underwater sound [3–5], and in investigations of low-energy underwater explosions [6]. They are also being used in modern industrial explosives for sensitizing purposes [7]. (In the last case they are of very small dimensions and are called microballoons).

During implosions or explosions of the hollow glass spheres in the liquids, freely oscillating bubbles are produced. In the experiments cited above a number of data on the wall motion of these bubbles and on the pressure waves radiated during their oscillations were collected. In this paper an estimation of the bubble oscillation intensities and of the associated energy losses will be presented on the basis of these data. For this purpose the procedure and results recently given in [8–10] will be used. The results obtained here are of interest not only because they throw more light on the experiments with imploding and exploding glass spheres, but also because they demonstrate rather clearly the difficulties current research on bubble dynamics is encountering in general (though, as will be shown in the paper, in the case of glass spheres the difficulties are increased by the presence of the glass fragments in the liquid).

Throughout the paper non-dimensional W and Z variables and certain energy relations and scaling functions will be used. The definitions of these quantities are to be found in Appendices A and B. The corresponding scaling functions are displayed in Ap-

Received 30 October 1988,
Accepted 12 November 1988.

K. Vokurka, Department of Physics, Faculty of Electrical Engineering, Czech Technical University, Prague.
Present address: Švédská 27, Jablonec n.N., CS-466 01, Czechoslovakia.

pendix B. Finally a list of nomenclature is given in Appendix C.

2. Experiments with pressurized glass spheres

When a pressurized thin-wall hollow glass sphere submerged in a water tank is shattered, a weak shock wave is radiated into the liquid and the released gas bubble begins oscillating. This technique was used by Heuckroth and Glass in a study of low-energy underwater explosions [6].

Let us consider the data displayed in Fig. 12 (runs SU-23 and SU-30) of [6]. In this particular case the radius of the glass sphere (the initial radius of the gas bubble) was $R_{m0} = 50.8$ mm (2 in), the non-dimensional initial pressure of the gas $P^*_{M0} = 20$, the ambient pressure in the liquid $p_\infty = 100$ kPa, the density of the liquid (water) $\varrho_\infty = 10^3\,\mathrm{kg\,m^{-3}}$ and the gas used was air (polytropic exponent $\gamma = 1.4$). According to the published data the released bubble expanded to a non-dimensional maximum radius $W_{M1} = 3.47$ and then contracted to a minimum radius $W_{m1} = 1.85$.

The authors also presented the theoretical time history of the bubble wall motion computed with Rayleigh's equation of motion. It can be seen that at the early stages of the bubble expansion, the theoretical curve agrees with the experimental points rather well. At the first maximum the theoretical value $W_{M1} = 3.35$ is slightly below the experimental points, and at later stages the deviation between the experiment and theory further increases. This deviation is attributed by the authors to the increased non-radial motion of the water brought about by the boundary surfaces of the small experimental tank [6].

The equilibrium radius of the bubble equals [11] $W_e = (P^*_{M0})^{1/3\gamma} = 2.04$. Hence the theoretical amplitude with which the bubble was excited to oscillate is $A_1 = W_{M1}/W_e = 1.64$ (here the theoretical value of $W_{M1} = 3.35$ was used). For a given pressure P^*_{M0} and exponent γ the amplitude could also be directly determined from the scaling function $A(P^*_M, \gamma)$ given in [10].

Let us now examine the compression phase. The theoretical value of W_{m1} corresponding to $A_1 = 1.64$ and $\gamma = 1.4$ is $W_{m1} = 1.05$. (This can be determined, for example, by using the scaling function $Z_m(A, \gamma)$ given in [8]. For given A_1 and γ one finds that the minimum radius is $Z_{m1} = 0.313$. Then $W_{m1} = Z_{m1}\,W_{M1}$.) However, the bubble does not contract to this theoretical minimum radius, but, as already pointed out, to a much larger value $W_{m1} = 1.85$. As can be verified (by means of the same approach as above but now in the reverse order) this radius corresponds to an amplitude $A_1 = 1.33$.

The partition of energies associated with the first bubble oscillation is summarised in Table I. The energies given in Table I were computed by means of the formulae from Appendix A. The experimental energy, E_{wsh}, was assumed to be the same as the theoretical one because it was found [9] that E_{wsh} is determined by the value of P^*_{M0} first of all and hence is little influenced by the energy losses at later stages. The energy E_{wbpl} can be determined from the function $E_{zbpl}(A, p_\infty)$ given in Fig. B3 in Appendix B. For $A = 1.33$ and $p_\infty = 100$ kPa one finds that $E_{zbpl} = 0.01\,E_{zpM1}$. Then $E_{wbpl} = 0.01\,E_{wpM1} = 0.01\,W^3_{M1}$.

Table I. Energy partition in the experiment with pressurized glass sphere [6] (the first oscillation).

		Theoretical values $A_1 = 1.66$, $W_{m1} = 1.05$		Experimental values $A_1 = 1.33$, $W_{m1} = 1.80$	
$W = W_{m0}$	E_{wiM0}	50	100%	50	100%
$W = W_{m1}$	E_{wiM1}	46.9	93.9%	23.9	47.8%
	ΔE_{wp}	0.2	0.3%	5.3	10.6%
	ΔE_{wd}	2.9	5.8%	20.8	41.6%
	ΔE_{wa}	2.9	5.8%	2.1	4.2%
	ΔE_{wu}	0	0 %	18.7	37.4%

As can be seen from Table I, approximately 37.4% of the initial internal energy was dissipated during the first bubble oscillation (above all during the compression phase) by a dissipative mechanism that was not taken into account in the theoretical model used to compute the scaling functions. In our opinion such a large energy dissipation cannot be attributed to the vertical motion of the bubble as suggested by Heuckroth and Glass [6]. First, for $A_1 = 1.64$ and the maximum radius $R_{M1} = 0.18$ m it is possible to determine in the bubble map (Fig. 6 in [12]) that the bubble considered belongs to the sizes of bubbles for which the effect of gravity should be negligible. Second, it is known that the influence of gravity is most pronounced in the vicinity of W_{m1} (see, e.g. [13]), and therefore the largest energy losses are also to be expected here. However, from the published data [6] it follows that significant energy losses occur immediately after W_{M1}.

It seems to us that the factor responsible for the unaccounted losses is a bubble wall distortion, and turbulence thus induced in the liquid. (The bubble wall distortion is due to the presence of the glass fragments surrounding the bubble.) This assumption is further supported by the analysis given in the following sections.

3. Experiments with explosive gaseous mixtures

Popov and Kogarko [5] describe an experiment in which they filled a hollow glass sphere of a volume

$V_{m0} = 60 \times 10^3$ mm^3 ($R_{m0} = 24$ mm) with an explosive gaseous mixture $2H_2 + O_2$. When the gas was detonated, the sphere was shattered, a weak shock wave was radiated into the surrounding liquid, and the released vapour bubble started oscillating. The authors registered a bubble wall motion and radiated pressure wave. The wave was picked up with a hydrophone placed at a distance from the bubble centre $r = 55$ mm. The experiment was performed in a water tank ($p_\infty = 100$ kPa, $\varrho_\infty = 10^3$ kg m^{-3}).

The observed bubble expanded to a maximum radius $R_{M1} = 53$ mm ($W_{M1} = 2.2$), then contracted to a first minimum radius $W_{m1} = 0.15 \cdots 0.3$ and again expanded to a second maximum radius $W_{M2} = 0.875$. The peak pressure in the shock wave was $p_{p0} = 440$ kPa, and the peak pressure in the first bubble pulse was approximately 2 to 4 times higher than p_{p0}, i.e. $p_{p1} = 880 \cdots 1760$ kPa. This is a rather well documented experiment. It is only seldom in the literature that the data on the bubble wall motion and radiated wave can be found together. Unfortunately, however, it is not clear from the text whether the two records belong to the same bubble.

The non-dimensional peak pressure in the shock wave as determined from the data given above is $p_{wp0} = (p_{p0}/p_\infty) r/R_{m0} = 10.1$. Thus the initial maximum pressure at the bubble wall equals $P^*_{M0} = p_{wp0} + 1 = 11.1$, and the equilibrium bubble radius for the growth phase is $W'_{e1} = (P^*_{M0})^{1/3\gamma} = 1.9$. (As the result of the chemical reaction the bubble contains water vapour, the polytropic exponent equals approximately [14] $\gamma = 1.25$.) The corresponding theoretical first maximum radius can be determined for given values of P^*_{M0} and γ from the scaling function $W_M(P^*_M, \gamma)$ given in [10]. One finds that $W_{M1} = 2.92$. Then the theoretical amplitude of the bubble oscillation for the growth phase is $A'_1 = W_{M1}/W'_{e1} = 1.54$. (This can also be determined directly from a function $A(P^*_M, \gamma)$ given in [10].) As the experimental first maximum radius is $W_{M1} = 2.2$, the experimental growth amplitude is $A'_1 = 1.16$.

A comparison of the theoretical and the experimental values of both W_{M1} and A'_1 reveals that in this experiment, in contrast to the previous example [6], energy losses occur already during the bubble growth. A detailed break-down of the energies for the growth phase is given in Table II. The experimental energy E_{wsh} was assumed to be again the same as the theoretical one.

Let us now evaluate the first collapse and rebound phase data. For this purpose the scaling functions $p_{zp}(A, \gamma)$, $Z_m(A, \gamma)$, $\alpha(A, \gamma)$, and $\Delta E_{za}(A, \gamma)$ given in [8] will be used and the evaluation will be performed in the Z-system of variables. The non-dimensional peak pressure in the first bubble pulse, $p_{zp1} = (p_{p1}/p_\infty) r/R_{M1}$, ranges from 9.1 to 18.3. Using the scaling function $p_{zp}(A, \gamma)$ one finds that for $\gamma = 1.25$ the corresponding collapse amplitude is $A''_1 = 1.88 \cdots 2.11$. The first minimum radius, $Z_{m1} = R_{m1}/R_{M1}$, ranges from 0.068 to 0.136 (the average value is $\langle Z_{m1} \rangle = 0.1$). Using the scaling function $Z_m(A, \gamma)$ one finds that $A''_1 = 2.07 \cdots 2.66$. (For the average minimum radius $\langle Z_{m1} \rangle = 0.1$ one obtains an average amplitude $\langle A''_1 \rangle = 2.25$). Finally, the first damping factor is $\alpha_1 = R_{M2}/R_{M1} = 0.40$. Using the function $\alpha(A, \gamma)$ one obtains $A''_1 = 6.4$.

Table II. Energy partition in the experiment with explosive gaseous mixture [5] (the growth phase).

		Theoretical values $A'_1 = 1.54$, $W_{M1} = 2.92$		Experimental values $A'_1 = 1.16$, $W_{M1} = 2.20$	
$W = W_{m0}$	E_{wiM0}	44.4	100%	44.4	100%
$W = W_{M1}$	E_{wim1}	16.9	44.8%	24.6	55.4%
	ΔE_{wp}	23.9	53.8%	9.7	21.7%
	ΔE_{wd}	0.6	1.4%	10.1	22.9%
	E_{wsh}	0.6	1.4%	0.6	1.4%
	ΔE_{wu}	0	0 %	9.5	21.5%

In a recent paper [14] it was shown that the collapse of a vapour bubble is governed by the amplitude $A''_1 = 3.29$. This amplitude is much larger than those determined here from experimental data on p_{zp1} and Z_{m1}, and much smaller than that determined from data on α_1. The reason for this discrepancy is again energy dissipation not accounted for by the theoretical model used to calculate the scaling functions. Popov and Kogarko [5] attribute the energy losses to heat conduction. Even though the influence of heat conduction cannot be completely excluded, in the author's opinion it does not play a decisive role (see, e.g., the bubble map in [12]). The interpretation suggested here is that the glass fragments surrounding the bubble distort the bubble wall and thus induce intensive turbulence. The resulting energy losses then slow down the collapse and limit the bubble regrowth. A detailed break-down of the energies for the collapse and rebound phases is given in Table III. In Table III the experimental minimum radius Z_{m1} and amplitude A''_1 are the average values as determined above.

Since an ideal vapour bubble is a non-equilibrium thermodynamic system, the simple energy formulae given in Appendix B are, strictly speaking, not applicable here. Nevertheless, to a first approximation the bubble can be treated as a gas bubble oscillating with a theoretical amplitude $A''_1 = 3.29$ [14] (the corresponding initial minimum pressure being $P^*_{m1} = 0.012$). Then, with respect to the specific behaviour of the

Table III. Energy partition in the experiment with explosive gaseous mixture [5] (the collapse and rebound phases).

		Theoretical values $A_1'' = 3.29$, $Z_{m1} = 0.03$, $Z_{M2} = 0.71$	Experimental values $\langle A_1'' \rangle = 2.25$, $\langle Z_{m1} \rangle = 0.10$, $Z_{M2} = 0.40$
$Z = Z_{M1}$	E_{zpM1}	100%	100%
$Z = Z_{m1}$	E_{zpm1}	0 %	0.1%
	ΔE_{zi}	60.6%	22.2%
	ΔE_{zd}	39.4%	77.7%
	E_{zbpl}	39.4%	11.5%
	ΔE_{zu}	0 %	66.2%
$Z = Z_{M2}$	E_{zpM2}	35.8%	6.4%
	ΔE_{zi}	1.4%	4.7%
	ΔE_{zd}	62.8%	88.9%
	E_{zbp}	62.8%	20.5%
	ΔE_{zu}	0 %	68.4%

vapour bubbles, the experimental energy E_{zim1} is assumed to be the same as the theoretical one. However, in determining further energies in Table III, the theoretical and experimental values of Z_{m1} and Z_{M2} are used to find the theoretical and experimental energies, respectively.

In determining the experimental values of E_{zbpl} and E_{zbp} it was assumed that the bubble oscillates like a gas bubble with the amplitude $A_1 = 2.25$ ($P_{m1}^* = 0.048$). The energy E_{zbpl} was then found in the usual manner described above ($\langle Z_{m1} \rangle = 0.1$). The energy E_{zbp} can be determined by means of the scaling function $\Delta E_{za}(A, \gamma)$ [8]. For $A = 2.25$ and $\gamma = 1.25$ one obtains $E_{zbp} = 0.205$.

A fact worth noting is the relation between R_{m0} and R_{m1}, and between p_{p0} and p_{p1}. For gas bubbles it is always true that $R_{m0} < R_{m1}$ and $p_{p0} > p_{p1}$ [10]. However, in the experiment considered it was found that $R_{m0} > R_{m1}$ and $p_{p0} < p_{p1}$. Popov and Kogarko [5] explain this "unusual" behaviour by heat losses from the gas bubble. In the author's opinion heat losses from the gas bubbles can increase the difference between R_{m0} and R_{m1}, and between p_{p0} and p_{p1}, but they cannot reverse the inequality sign. However, as has been mentioned above, the bubble produced in this experiment is a vapour bubble and as dicussed elsewhere [15] the relations $R_{m0} > R_{m1}$ and $p_{p0} < p_{p1}$ are rather typical of vapour bubbles.

4. Experiments with imploding glass spheres

When a partially evacuated hollow glass sphere is shattered in water, the gas contained in the sphere is compressed by the liquid and the bubble thus generated performs several oscillations. During each bubble compression a pressure pulse (bubble pulse) is radiated into the liquid. Orr and Schoenberg [4] used implosions of such spheres as simple, inexpensive, deep-underwater, wide-band sound sources.

The two authors used glass spheres of a radius R_{M1} (initial radius of the gas bubbles) ranging from 117.5 to 216 mm. The spheres imploded at various depths in the ocean (i.e. under various ambient pressures p_∞) and the authors registered the radiated pressure waves. The captured waveforms are displayed in [4]. The authors also give in a tabular form (Tables I and II in [4]) the numerical values of the peak pressure $p_{p1} = p_{M1} - p_\infty$, of the trough pressure $p_{v1} = p_{m1} - p_\infty$ (p_{M1} and p_{m1} are the maximum and minimum pressures in the wave, respectively, and the values of p_{p1} and p_{v1} are converted to a distance $r = 1$ m from the bubble centre), of the energy stored in the wave, ΔE_a, and of the characteristic time intervals T_1, T_2, T_3, and T_4.

As a concrete example let us consider the sphere No. 1 in [4]. The values recorded for this particular sphere are summarised in Table IV. In this table P_{m1} is the initial pressure at the bubble when $R = R_{M1}$ (the gas pressure in the evacuated sphere). The compression time, T_{c1}, was computed from the characteristic time intervals as follows: $T_{c1} = T_1 + T_2 + T_3/2$.

From these data the non-dimensional peak pressure is $p_{zp1} = 1.77$. A theoretical variation of p_{zp} with A is displayed in Fig. B2 (Appendix B). For $p_{zp1} = 1.77$ and $p_\infty = 30$ MPa one can find that the corresponding amplitude is $A_1 = 1.55$. This is a very low am-plitude when compared with the theoretical one $A_1 = (P_{m1}^*)^{-1/3\gamma} = 4.41$ [11]. It is assumed that such a drop in the intensity of the bubble oscillation is due, as before, to the distortion of the bubble surface by the glass fragments and the associated turbulence.

The non-dimensional trough pressure for sphere No. 1 is $p_{zv1} = (p_{v1}/p_\infty) r/R_{M1} = -0.36$. Then the minimum pressure at the bubble wall is equal to $P_{m1}^* = p_{zv1} + 1 = 0.64$. The corresponding amplitude is $A_1 = (P_{m1}^*)^{-1/3\gamma} = 1.11$. This is an even lower value of A_1 than that determined from p_{zp1}. The reason for this has perhaps to be seen in the fact that the trough pressure p_{v1} occurs not at the beginning of the compression phase (as required by the relation for P_{m1}^* used to compute A_1) but approximately at the time $\sim \frac{2}{3} T_{c1}$, when the acoustic pressure is already smaller.

Table IV. Experimental data on sphere No. 1 (Ref. [4]).

R_{M1} mm	p_∞ MPa	P_{m1} kPa	γ	r m	p_{p1} MPa	p_{v1} MPa	T_{c1} ms	ΔE_a MJ
216	35.5	70	1.4	1	13.6	−2.76	1.95	0.288

This shift in the occurrence of p_{v1} (and hence in the value of p_{v1}) is most probably also due to the presence of the glass fragments.

The non-dimensional acoustic energy equals $\Delta E_{za} = \Delta E_a / E_{pM1} = 0.192$. For this value of $\Delta E_{za} \doteq E_{zbp}$ Fig. B4 shows that the corresponding amplitude is $A_1 = 1.30$ ($p_\infty = 30$ MPa).

The non-dimensional compression time is $T_{zc1} = T_{c1}/[R_{M1}(\varrho_\infty/p_\infty)^{1/2}] = 1.70$. This value is even larger than the theoretical compression time of bubbles oscillating with an amplitude $A \to 1$. (In this case the compression time is a maximum and equals $T_{zc1} = \pi/(3\gamma)^{1/2} = 1.53$ [16].) This again indicates that the bubble compression is strongly slowed down by the glass fragments.

The energy partition for sphere No. 1 is given in Table V. The experimental amplitude A_1 in Table V was determined from the peak pressure p_{zp1}, and the corresponding value of Z_{m1} was found for this A_1 and $p_\infty = 30$ MPa in Fig. B1. However, for determining the experimental energy E_{zbp1} we made use of the amplitude A_1, as determined from ΔE_{za} above. Then for $A_1 = 1.30$ and $p_\infty = 30$ MPa Fig. B3 gives $E_{zbp1} = 0.12$. The theoretical value of Z_{m1} in Table V was computed by means of Herring's simplified equation of motion for the pressures $P_{m1} = 70$ kPa and $p_\infty = 35.5$ MPa.

From Table V it follows that the energy dissipated during the bubble compression amounts to as much as 87% and 90.6% of the available initial potential energy for the theoretical and experimental bubbles, respectively. However, whereas in the theoretical bubble, dissipation is due to acoustic radiation only; in the experimental bubble only a fraction of the dissipated energy is carried away by the leading edge of the bubble pulse. In the latter case most of the energy is dissipated by an unknown mechanism (most probably turbulence).

The large energy dissipation has interesting consequences. First, as there is only fraction of the initial energy left for further oscillations the intensity of successive oscillations is very small. Hence in the displayed waveforms (Fig. 5 in [4]) the first bubble pulse dominates the picture. (One can also notice minute peaks for later times. These are, most probably, the second, third, and further bubble pulses.) Second, due to high energy dissipation a saturation can be observed in experimental data: even if the amplitude A_1 is further increased, the radiated energy grows only insignificantly. For example, sphere No. 1 was evacuated to a pressure $P_{m1} = 70$ kPa ($A_1 = 4.41$) and sphere No. 4 to a pressure $P_{m1} = 7$ kPa ($p_\infty = 32.6$ MPa, hence $A_1 = 7.47$). Though the theoretical amplitude was much higher in the second case, no distinct difference can be seen in the recorded values of ΔE_{za} (see [4]).

Table V. Energy partition in the experiment with imploding evacuated sphere [4] (the compression phase).

		Theoretical values $A_1 = 4.41$ $Z_{m1} = 0.06$	Experimental values $A_1 = 1.55$ $Z_{m1} = 0.44$
$Z = Z_{M1}$	E_{zpM1}	100%	100%
$Z = Z_{m1}$	E_{zpm1}	0 %	8.6%
	ΔE_{ziM1}	12.9%	0.8%
	ΔE_{zd}	87.0%	90.6%
	E_{zbp1}	87.0%	12.0%
	ΔE_{zu}	0 %	78.6%

Even earlier experiments of this sort were reported by Urick [3] who used ordinary air-filled glass bottles sealed merely by screwing on their plastic caps. As an example let us evaluate a waveform produced by a one-pint bottle ($V_{M1} = 0.473 \times 10^{-3}$ m^{-3}; radius of an equivalent spherical volume $R_{M1} = 48.3$ mm) imploding at a depth $h = 390$ m ($h = 1280$ ft; $p_\infty = 4$ MPa). The waveform is displayed in Fig. 1 of [3]. The values of several quantities estimated from the displayed waveform are summarised in Table VI where r is the difference between the implosion depth of 390 m (1280 ft) and the depth of the receiving hydrophone of 15.5 m (50 ft).

Table VI. Experimental data on one-pint bottle [3].

R_{M1} mm	p_∞ MPa	P_{m1} kPa	γ	r m	p_{p1} Pa	p_{v1} Pa	T_{c1} ms	β_1
48.3	4	100	1.4	375	220	−100	1.78	0.25

The non-dimensional peak pressure in this example is $p_{zp1} = 0.43$. The corresponding amplitude as determined from Fig. B2 for $p_\infty = 3$ MPa is $A_1 = 1.13$. This is a lower value than that determined from the data of Orr and Schoenberg [4]. The reasons for the lower intensity of bubble oscillations may be two. First, it is the non-spherical form of the bottle which decreases the intensity and, second, there is a lower theoretical amplitude $A_1 = 2.41$.

Similar lower values of the amplitude are found when evaluating the trough pressure. In this case $p_{zv1} = -0.19$, $P^*_{m1} = 0.81$, and hence $A_1 = 1.05$. In the case of the compression time, an excessively large value is determined again, i.e. $T_{zc1} = 2.33$. One should also notice the very low value of the damping factor $\beta_1 = T_{o2}/T_{o1} = 0.25$ [8] (here $T_{o1} \doteq 2\,T_{c1}$; T_{o1} and T_{o2} being the times of the first and second bubble oscillations). The energy partition for this experiment is

Table VII. Energy partition in the experiment with imploding one-pint bottle [3] (the compression phase).

		Theoretical values $A_1 = 2.41$ $Z_{m1} = 0.14$	Experimental values $A_1 = 1.13$ $Z_{m1} = 0.78$
$Z = Z_{M1}$	E_{zpM1}	100%	100%
$Z = Z_{m1}$	E_{zpm1}	0.3%	47.5%
	ΔE_{ziM1}	58.1%	2.2%
	ΔE_{zd}	41.6%	50.3%
	E_{zbpl}	41.6%	1.7%
	ΔE_{zu}	0 %	48.6%

given in Table VII. In this table the experimental acoustic energy E_{zbpl} was determined from Fig. B 3 on the basis of $A_1 = 1.13$ and $p_\infty = 3$ MPa.

In model experiments on sonoluminescence Schmid [1] and Müller [2] used evacuated Christmas-tree glass balls. For example, in Fig. 2 in [1] Schmid gives a record taken by high-speed photography of an imploding sphere having an initial radius $R_{M1} = 35$ mm. This sphere was evacuated to a pressure $P_{m1} = 3.2$ kPa (24 torr). As in this case $p_\infty = 100$ kPa and $\gamma = 1.4$ (air), the theoretical amplitude is $A_1 = 2.27$. Schmid determined that the compression time equalled $T_{c1} = 4$ ms. As this particular experiment was performed in water ($\varrho_\infty = 10^3$ kg m^{-3}), the non-dimensional compression time is $T_{zc1} = 1.14$. By means of the scaling function $T_{zc}(A, \gamma)$ given in [8] one finds that this compression time corresponds to an experimental amplitude $A_1 = 1.42$. Note that in contrast to the previous experiments [3, 4] the compression time can now be used to determine the amplitude A_1, and the value of A_1 agrees rather well with previous findings. From Fig. 2 of [1] it also follows that the compression was highly non-symmetrical. Similar conclusions can be drawn from investigation of Müller [2]. Both researchers have also reported a large scatter of experimental data. This scatter is to be attributed to the randomly acting dissipative mechanism that is induced by the non-symmetric highly distorted bubble compression.

5. Discussion and conclusion

The evaluation of the available experimental data on imploding and exploding hollow glass spheres in liquids revealed excessive dissipation of energy and greatly reduced amplitudes of bubble oscillations. The results found are summarised in Table VIII. It shows that the unaccounted energy losses ΔE_{zu} grow with the theoretical amplitude of the oscillations A_1. Also worth noting is that all the bubbles belong to the category of scaling bubbles, i.e. the effects of gravity, surface tension, viscosity, and heat conduction should be insignificant for them.

If one considers the purposes for which the glass spheres are used one can distinguish two groups. The first group encompasses applications which require high maximum temperatures at bubble compression, θ_{M1}. To this group belong the experiments of Schmid [1], Müller [2], and the use of microballoons in industrial explosives [7]. The second group encompasses applications where high acoustic radiation ΔE_a is required. To this group belong the experiments of Urick [3], Orr and Schoenberg [4], and Popov and Kogarko [5].

From the energy partition results and from Table VIII it follows that in order to obtain high θ_{M1} and high ΔE_a it is necessary to use as high theoretical amplitudes A_1 as possible, and to minimize the energy losses ΔE_u. As far as the amplitude is concerned this requires either highly evacuated spheres ($P_{m1} \to P_v$, where P_v is the liquid vapour pressure) or vapour bubbles (produced by explosive mixtures $2H_2 + O_2$). The second way of achieving high amplitudes is to use high ambient pressures p_∞. As far as ΔE_u is concerned, it is evident that the glass vessel should be spherical. However, further experiments are needed to determine the optimum form of the glass fragments (e.g. many small splinters or few large pieces, etc.).

From Figs. B 3 and B 4 and Table VIII one can see that acoustic radiation grows in direct proportion with A_1 and p_∞. Hence, as a second requirement for obtaining high θ_{M1} it is necessary to keep p_∞ as low as possible. On the other hand to obtain a high ΔE_a, the ambient pressure p_∞ should be as high as possible.

Table VIII. Comparison of experiments with imploding and exploding glass spheres.

Authors	R_{M1} mm	γ	p_∞ MPa	A_1 theoretical	A_1 experimental	ΔE_{zu} (compression phase)	E_{zbpl}
H + G [6]	176.3	1.4	0.1	1.64	1.33	37.4%	0.8%
U [3]	48.3	1.4	4.0	2.41	1.13	48.6%	1.7%
P + K [5]	53	1.25	0.1	3.29	2.25	66.2%	11.5%
O + S [4]	216	1.4	35.5	4.41	1.55	78.6%	12.0%

Because of our findings the results published by Schmid [1] and Müller [2] can be seen in a new light. The amplitude $A_1 = 1.42$, for example, found here for Schmid's experiment corresponds to a minium radius $Z_{m1} = 0.45$. Hence the maximum temperature of the gas in this experiment was approximately $\theta_{M1} = \theta_\infty Z_{m1}^{-3(\gamma-1)} = 764$ K ($\gamma = 1.4$, temperature of the liquid $\theta_\infty = 293$ K). This is a much lower value than the one assumed by Schmid [1] and Müller [2]. Thus it supports the findings of Crum and Reynolds [17] that sonoluminescence can be observed even for moderate intensities of bubble oscillations.

It goes without saying that the results presented here represent first approximations only. The main sources of inaccuracies are the scaling functions used to determine the amplitudes of oscillation, minimum bubble radii, etc. The reason for this is that these functions have been calculated with bubble models that do not take into account energy dissipation due to bubble wall distortion. Even if there are uncertainties regarding the exact values of the computed quantities, we believe that the results are valid in a general sense.

As discussed elsewhere [8], an oscillating bubble is described by two parameters. These are the bubble size and the amplitude of the oscillations. However, in the light of the results presented here it seems that if we are to arrive at a more exact description of the real bubble a further parameter is needed characterizing the degree of the bubble wall distortion. We suggest calling this new parameter a distortion factor, ε, and to define its numerical value as the ratio of the unaccounted energy ΔE_u to the initial bubble energy. (As the initial energy we have considered E_{wiM} or E_{zpM} in the W or Z systems, respectively.) As follows from Table VIII, the distortion factors computed here for the first compression or collapse phases, ε_{c1}, range from 0.37 to 0.79. It is hoped that the glass spheres could be used to produce oscillating bubbles with a prescribed degree of distortion (e.g. by varying the size and form of the glass fragments), and that these unusual bubbles could subsequently be used for mapping the bubble behaviour.

Appendix A: Expansion system

In the expansion system of variables the non-dimensional radius, time, energy, pressure at the bubble wall, and peak pressure in the wave at a point r in the liquid are defined as

$$W = R/R_{m0},\ t_w = t/[R_{m0}(\varrho_\infty/p_\infty)^{1/2}],\ E_w = E/E_{pm0},$$
$$P^* = P/p_\infty,\ p_{wp} = (p_p/p_\infty)r/R_{m0}.$$

Here R_{m0} is the initial bubble radius, ϱ_∞ the liquid density, p_∞ the ambient pressure in the liquid, and $E_{pm0} = \frac{4}{3}\pi p_\infty R_{m0}^3$ the potential energy of the liquid when $R = R_{m0}$.

The energy relation in the expansion system can be written as

$$\Delta E_{wi} = \Delta E_{wp} + E_{wk} + \Delta E_{wd} \tag{A1}$$

where the initial internal energy of the gas (referred to infinite adiabatic expansion) equals

$$E_{wiM0} = \frac{P_{M0}^*}{\gamma - 1} \tag{A2}$$

Here P_{M0}^* is the initial (maximum) gas pressure and γ the polytropic exponent of the gas. For a wall position W the internal energy is

$$E_{wi} = E_{wiM0} W^{-3(\gamma-1)} \tag{A3}$$

and hence the change in the internal energy during the wall motion from W_{m0} to W equals

$$\Delta E_{wi} = E_{wiM0} - E_{wi} \tag{A4}$$

The change in the potential energy of the liquid is given by

$$\Delta E_{wp} = W^3 - 1 \tag{A5}$$

Finally E_{wk} and ΔE_{wd} designate the kinetic and dissipated energy, respectively. When $W = W_m$ and $W = W_M$ it can be assumed that the kinetic energy $E_{wk} \doteq 0$.

The dissipated energy equals

$$\Delta E_{wd} = \Delta E_{wa} + \Delta E_{wu} \tag{A6}$$

where ΔE_{wa} is the radiated acoustic energy and ΔE_{wu} encompasses all other energy losses. Theoretical acoustic energies carried away by the shock wave, E_{wsh}, and the leading edge of the bubble pulse, E_{wbpl}, can be determined from eq. (A1) using the theoretical values of W_{M1} and W_{m1}, respectively. As acoustic losses only are considered in our theoretical model, then $\Delta E_{wu} = 0$. Hence, when $W = W_{M1}$, $\Delta E_{wd} = E_{wsh}$. In the second case ($W = W_{m1}$) $\Delta E_{wd} = \Delta E_{wa}$, where the total acoustic energy radiated up to W_{m1} equals

$$\Delta E_{wa} = E_{wsh} + E_{wbpl} \tag{A7}$$

The experimental energies are computed in the same way, but now $\Delta E_{wu} \neq 0$ and the experimental radii W_{M1} and W_{m1} have to be used.

Appendix B: Compression system

In the compression system of variables the non-dimensional radius, time, energy, pressure at the bubble wall, and the acoustic pressure in the wave at a point

r in the liquid are defined as

$$Z = R/R_{M1}, \quad t_z = t/[R_{M1}(\varrho_\infty/p_\infty)^{1/2}], \quad E_z = E/E_{pM1}$$
$$P^* = P/p_\infty, \quad p_{za} = (p_a/p_\infty) r/R_{M1}$$

Here R_{M1} is the first maximum bubble radius, $E_{pM1} = \frac{4}{3}\pi p_\infty R_{M1}^3$ the potential energy of the liquid when $R = R_{M1}$, $p_a = p - p_\infty$ the acoustic pressure, and p the absolute pressure in the wave.

The energy relation in the compression system can be written as

$$\Delta E_{zp} = \Delta E_{zi} + E_{zk} + \Delta E_{zd} \tag{B1}$$

where the change in the potential energy of the liquid is given by

$$\Delta E_{zp} = E_{zpM1} - E_{zp} \tag{B2}$$

It follows from the definition of the energies that $E_{zpM1} = 1$ and $E_{zp} = Z^3$. The internal energy of the gas when $Z = Z_{M1} = 1$ (referred to infinite adiabatic expansion) equals

$$E_{zim1} = \frac{P_{m1}^*}{\gamma - 1} \tag{B3}$$

Here P_{m1}^* is the initial (minimum) pressure at the bubble wall. For a wall position Z the internal energy is

$$E_{zi} = E_{zim1} Z^{-3(\gamma-1)} \tag{B4}$$

and hence the change in the internal energy during the wall motion from Z_{M1} to Z equals

$$\Delta E_{zi} = E_{zi} - E_{zim1} \tag{B5}$$

Finally E_{zk} and ΔE_{zd} designate the kinetic and dissipated energy, respectively. When $Z = Z_M$ and $Z = Z_m$ it can be assumed that the kinetic energy $E_{zk} \doteq 0$.

The dissipated energy equals

$$\Delta E_{zd} = \Delta E_{za} + \Delta E_{zu} \tag{B6}$$

where ΔE_{za} is the radiated acoustic energy and ΔE_{zu} encompasses all other energy losses. The theoretical acoustic energy carried away by the leading edge of

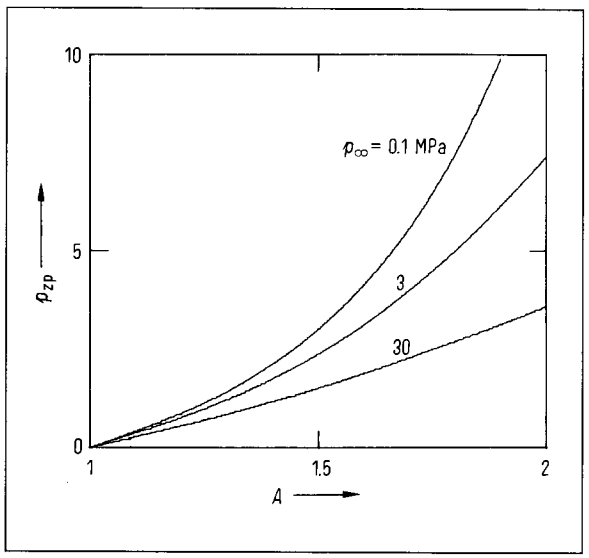

Fig. B2. Variation of the bubble pulse peak pressure, p_{zp}, with the amplitude of bubble oscillations, A, for different ambient pressures, p_∞ ($\gamma = 1.4$).

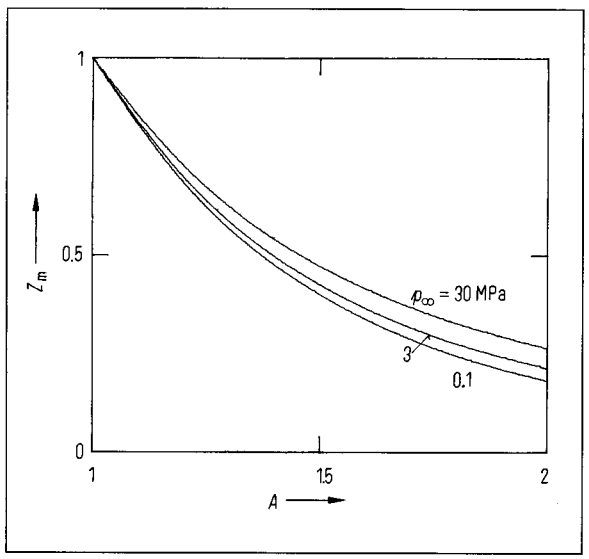

Fig. B1. Variation of the minimum bubble radius, Z_m, with the amplitude of bubble oscillations, A, for different ambient pressures, p_∞ ($\gamma = 1.4$).

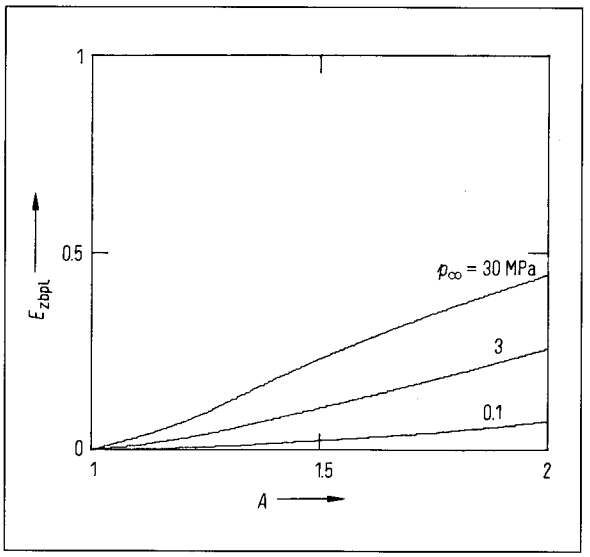

Fig. B3. Variation of the acoustic energy carried away by the leading edge of the bubble pulse, E_{zbpl}, with the amplitude of bubble oscillations, A, for different ambient pressures, p_∞ ($\gamma = 1.4$).

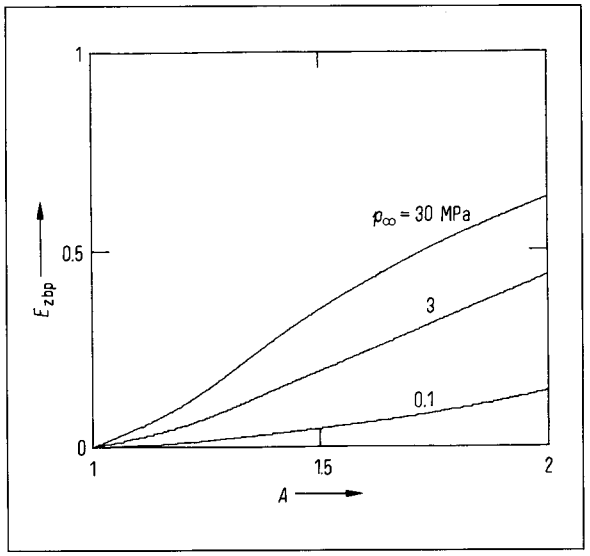

Fig. B4. Variation of the acoustic energy carried away by the bubble pulse, E_{zbp}, with the amplitude of bubble oscillations, A, for different ambient pressures, p_∞ ($\gamma = 1.4$).

the bubble pulse, E_{zbpl}, or by the whole bubble pulse, E_{zbp}, can be determined from eq. (B1) for $Z = Z_{m1}$ and $Z = Z_{M2}$, respectively. As in our theoretical model the only energy losses considered are acoustic, then $\Delta E_{zu} = 0$. Hence $\Delta E_{zd} = E_{zbpl}$ in the first case, and $\Delta E_{zd} = E_{zbp}$ in the second case. The experimental values can be computed in the same way but now $\Delta E_{zu} \neq 0$ and Z_{m1} and Z_{M1} are the experimental radii.

In order to facilitate the evaluation of the experimental data it is necessary to determine the theoretical variations of the minimum radius, Z_m, of the peak pressure in the bubble pulse, p_{zp}, and of the energies E_{zbpl}, and E_{zbp}, with the amplitude of the bubble oscillations A for different values of p_∞. The computed variations are given in Figs. B1 to B4. The computations were performed with the simplified Herring's equation of motion using the procedure described in detail in [8].

Appendix C: Nomenclature

In the list of nomenclature the first symbols denote dimensional quantities and the following ones non-dimensional quantities. The numbers in subscripts (omitted in the nomenclature but used in the text) denote the oscillation period, with zero denoting the initial values in the expansion system. In the case of vapour bubbles one apstrophe denotes the growth and rebound phases, and two apostrophes the collapse phase; (the apostrophes are also omitted in the list of nomenclature).

t, t_z, t_w	time
T_c, T_{zc}, T_{wc}	collapse or compression time
T_o, T_{zo}, T_{wo}	time of oscillation
R, Z, W	bubble radius
R_M, Z_M, W_M	maximum radius
R_m, Z_m, W_m	minimum radius
R_e, Z_e, W_e	equilibrium radius
E, E_z, E_w	energy
$E_p, E_{zp}, \Delta E_{zp}, E_{wp}, \Delta E_{wp}$	potential energy
E_{pM}, E_{zpM}, E_{wpM}	maximum potential energy
E_{pm}, E_{zpm}, E_{wpm}	minimum potential energy
$E_i, E_{zi}, \Delta E_{zi}, E_{wi}, \Delta E_{wi}$	internal energy
E_{iM}, E_{ziM}, E_{wiM}	maximum internal energy
E_{im}, E_{zim}, E_{wim}	minimum internal energy
E_k, E_{zk}, E_{wk}	kinetic energy
$\Delta E_d, \Delta E_{zd}, \Delta E_{wd}$	dissipated energy
$\Delta E_a, \Delta E_{za}, \Delta E_{wa}$	acoustic energy
E_{sh}, E_{zsh}, E_{wsh}	energy in the shock wave
E_{bp}, E_{zbp}, E_{wbp}	energy in the bubble pulse
$E_{bpl}, E_{zbpl}, E_{wbpl}$	energy in the leading edge of the bubble pulse
$\Delta E_u, \Delta E_{zu}, \Delta E_{wu}$	unaccounted energy
P, P^*	pressure at the bubble wall
P_M, P_M^*	maximum pressure at the wall
P_m, P_m^*	minimum pressure at the wall
P_v, P_v^*	liquid vapour pressure
p	pressure in the liquid
p_M	maximum pressure in the liquid
p_m	minimum pressure in the liquid
p_∞	ambient pressure in the liquid
p_a, p_{za}, p_{wa}	acoustic pressure in the wave
p_p, p_{zp}, p_{wp}	peak pressure in the wave
p_v, p_{zv}, p_{wv}	trough pressure in the wave
c_∞, c_∞^*	speed of sound in the liquid
A	amplitude of oscillation
ϱ_∞	liquid density
r	point in the liquid
γ	polytropic exponent
α	damping factor
β	damping factor
V_M	maximum volume of the bubble
V_m	minimum volume of the bubble
h	depth in the ocean
ε	distortion factor
ε_c	distortion factor for the collapse phase
θ_∞	ambient temperature
θ_M	maximum temperature
$\langle\ \rangle$	average value

References

[1] Schmid, J., The gas content and luminescence of a cavitation bubble (model experiments with glass spheres). Acustica **12** [1962], 70–83 (in German).

[2] Müller, H. M., Experiments on light emission from bubbles imploding in liquids (model experiments on sonoluminescence). Acustica **16** [1965/66], 22–33 (in German).
[3] Urick, R. J., Implosions as sources of underwater sound. J. Acoust. Soc. Amer. **35** [1963], 2026–2027.
[4] Orr, M. and Schoenberg, M., Acoustic signatures from deep water implosions of spherical cavities. J. Acoust. Soc. Amer. **59** [1976], 1155–1159.
[5] Popov, O. E. and Kogarko, S. M., One special feature of an underwater explosion of gas-mixtures. Fiz. Goreniya i Vzryva **12** [1976], 610–614 (in Russian) [English transl.: Combust. Explos. & Shock Waves **12** [1976], 554–558].
[6] Heuckroth, L. E. and Glass, I. I., Low-energy underwater explosions. Phys. Fluids **11** [1968], 2095–2107.
[7] Sudweeks, W. B., Physical and chemical properties of industrial slurry explosives. Ind. Eng. Chem. Prod. Res. Dev. **24** [1985], 432–436.
[8] Vokurka, K., A method for evaluating experimental data in bubble dynamics studies. Czech. J. Phys. **B 36** [1986], 600–615.
[9] Vokurka, K., Oscillations of gas bubbles generated by underwater explosions. Acta Technica ČSAV **27** [1987], 162–172.
[10] Vokurka, K., Excitation of gas bubbles for free oscillations by increasing their energy. J. Sound Vib. **116** [1987], 483–490.
[11] Vokurka, K., Excitation of gas bubbles for free oscillations. J. Sound Vib. **106** [1986], 275–288.
[12] Vokurka, K., The scaling law for free oscillations of gas bubbles. Acustica **60** [1986], 269–276.
[13] Cole, R. H., Underwater explosions. Princeton University Press, Princeton 1948, chapters 8.5 and 8.6.
[14] Vokurka, K., A simple model of a vapor bubble. J. Acoust. Soc. Amer. **81** [1987], 58–61.
[15] Vokurka, K., A model of spark and laser generated bubbles. Czech. J. Phys. **B 38** [1988], 27–34.
[16] Vokurka, K., On Rayleigh's model of a freely oscillating bubble. II. Results. Czech. J. Phys. **B 35** [1985], 110–120.
[17] Crum, L. A. and Reynolds, G. T., Sonoluminescence produced by "stable" cavitation. J. Acoust. Soc. Amer. **78** [1985], 137–139.